

The stellar content of the Hamburg/ESO survey*

II. A large, homogeneously-selected sample of high latitude carbon stars

N. Christlieb¹, P.J. Green², L. Wisotzki³, and D. Reimers¹

¹ Hamburger Sternwarte, Universität Hamburg, Gojenbergsweg 112, D-21029 Hamburg, Germany
e-mail: nchristlieb@hs.uni-hamburg.de

² Harvard-Smithsonian Center for Astrophysics, 60 Garden Street, Cambridge, MA 02140, USA
e-mail: pgreen@cfa.harvard.edu

³ Institut für Physik, Universität Potsdam, Am Neuen Palais 10, D-14469 Potsdam, Germany
e-mail: lutz@astro.physik.uni-potsdam.de

Received 26-April-2001; accepted 11-June-2001

Abstract. We present a sample of 403 faint high latitude carbon (FHLC) stars selected from the digitized objective prism plates of the Hamburg/ESO Survey (HES). Because of the $\sim 15 \text{ \AA}$ spectral resolution and high signal-to-noise ratio of the HES prism spectra, our automated procedure based on the detection of C_2 and CN molecular bands permits high-confidence identification of carbon stars without the need for follow-up spectroscopy. From a set of 329 plates (87% of the survey), covering $6\,400 \text{ deg}^2$ to a magnitude limit of $V \sim 16.5$, we analyze the selection efficiency and effective surface area of the HES FHLC survey to date. The surface density of FHLC stars that we detect ($0.072 \pm 0.005 \text{ deg}^{-2}$) is 2–4 times higher than that of previous objective prism and CCD surveys at high galactic latitude, even though those surveys claimed a limiting magnitude up to 1.5 magnitudes fainter. This attests to the highest selection sensitivity yet achieved for these types of stars.

Key words. Stars:carbon – Surveys – Galaxy:halo

1. Introduction

Models of the chemical and dynamical properties of the Galactic spheroid (the ‘halo’) are still rather weakly constrained. In the grand scheme, did a monolithic protogalaxy undergo rapid collapse and enrichment (Eggen et al. 1962), or did many smaller dwarf galaxies merge together (Searle & Zinn 1978)? Both processes probably contribute, since there is solid recent evidence of ongoing mergers (Ibata et al. 1994; Majewski et al. 2000). Stars and gas that are tidally stripped from accreting dwarf galaxies remain aligned with the orbit of the satellite for timescales comparable to the age of the Galaxy. Thus, a number of tidal streams exist today whose phase-space signature can constrain the stripping and merging events that contribute to the present-day galactic halo (Johnston et al. 1999).

An important goal of astronomy in this century is to measure and model the potential of the Milky Way us-

ing halo stars as tracers. To simultaneously disentangle the remnants of disrupted satellites requires full knowledge of the angular positions, proper motions, radial velocities, and distances of a large number of such stars. But first, a large sample of distant halo stars must be amassed. Intrinsically bright stars visible to large galactocentric distances (10–100 kpc) provide the best opportunity. Because they are readily recognizable from their strong C_2 and CN absorption bands, and because they were thought to be giants without exception, faint C stars have been sought as excellent tracers of the outer halo.

Faint high galactic latitude carbon (FHLC) stars have been sought in prior objective prism surveys (e.g., Sanduleak & Pesch 1988; MacAlpine & Lewis 1978) and in the CCD survey of Green et al. (1994). Objective-prism photography with wide-field Schmidt telescopes has yielded low-dispersion spectra for thousands of objects over substantial portions of the sky, but not a large number of carbon stars. Fewer than 1% of the 6 000 stars in Stephenson’s (1989) catalogue are the faint, high-latitude carbon (FHLC) stars ($V > 13$, $|b| > 40^\circ$) most useful as dynamical probes of the outer halo. The two most prolific sources of published FHLC stars, the Case low-dispersion survey (CLS; Sanduleak & Pesch 1988) and the University

Send offprint requests to: nchristlieb@hs.uni-hamburg.de

* Based on observations collected at the European Southern Observatory, Chile (Proposal IDs 145.B-0009 and 63.L-0148). Table B.1 is only available in electronic form at the CDS via anonymous ftp to [cdsarc.u-strasbg.fr](ftp://cdsarc.u-strasbg.fr) (130.79.125.5) or via <http://cdsweg.u-strasbg.fr/Abstract.html>.

of Michigan – Cerro Tololo survey (UM; MacAlpine & Williams 1981) appear to probe to about $V = 16$ and have provided about 30 FHLC stars. Emission-line objects, not FHLC stars, were the primary goal of these photographic surveys, and known FHLC stars were not examined to help predefine selection criteria or estimate completeness. The surface density of FHLC stars from objective-prism surveys is low, about one per 50 deg² to $V \approx 16$. At high galactic latitudes, mostly warm carbon stars are found – CH stars, and possibly some R stars. However, color selection of very red stars at high latitude also reveals a small number (one per 200 deg² to $R \sim 16$) of classical intermediate age AGB carbon (AGBC) stars (Totten & Irwin 1998). Margon et al. (2000) recently reported the discovery of more than 30 new FHLC stars in the commissioning data of the Sloan Digitized Sky Survey (SDSS), which may eventually provide the majority of known FHLC stars.

In this paper, we describe our use of the Hamburg/ESO survey (HES; Wisotzki et al. 1996; Reimers & Wisotzki 1997; Wisotzki et al. 2000) to greatly augment the number of known FHLC stars. The HES is an objective-prism survey designed to select bright ($12.5 \gtrsim B_J \gtrsim 17.5$) quasars in the southern extragalactic sky ($\delta < +2.5^\circ$; $|b| \gtrsim 30^\circ$). It is based on IIIa-J plates taken with the 1 m ESO Schmidt telescope and its 4° prism, yielding a wavelength range of $3200 \text{ \AA} < \lambda < 5200 \text{ \AA}$ and a seeing-limited spectral resolution of typically 15 Å at H γ . This resolution makes possible the identification of carbon stars with high confidence without follow-up slit spectroscopy, based on their strong C₂ and CN molecular bands (cf. Fig. 1).

Since carbon can reach the surface of an isolated star only in late evolutionary stages, it has long been assumed that all carbon (C) stars are giants. Due to their high luminosity ($M_R \sim -3.5$), it is possible to detect the red AGB stars at large distances: Brewer et al. (1996) have identified C stars even in the local group galaxy M31. The more typical FHLC stars such as CH giants, with $0 < M_V < -2.5$, can be detected to ~ 60 kpc in sensitive photographic surveys. However, the long-held assumption that all C stars are giants has fallen. Trigonometric parallax measurements for the carbon star G77–61 (Dahn et al. 1977) showed that this star lies close to the main sequence ($M_V \sim +10$). For years, the dwarf carbon (dC) stars phenomenon was assumed to be extremely rare until many new dCs were discovered in the early 1990s (Green et al. 1991, 1992; Warren et al. 1993; Heber et al. 1993; Liebert et al. 1994). Discovery of so many dCs, and the remarkable similarity of their spectra to those of C giants means that care must be taken to distinguish dwarfs from giants in FHLC star samples intended for distant halo studies (Green et al. 1992). We are therefore undertaking a two-part investigation. In the current paper, we describe our automated selection of C stars in the HES, and we present a large, uniformly selected, and flux-limited sample of FHLC stars. We complement this sample in upcoming work with recent epoch astrometry, to measure proper

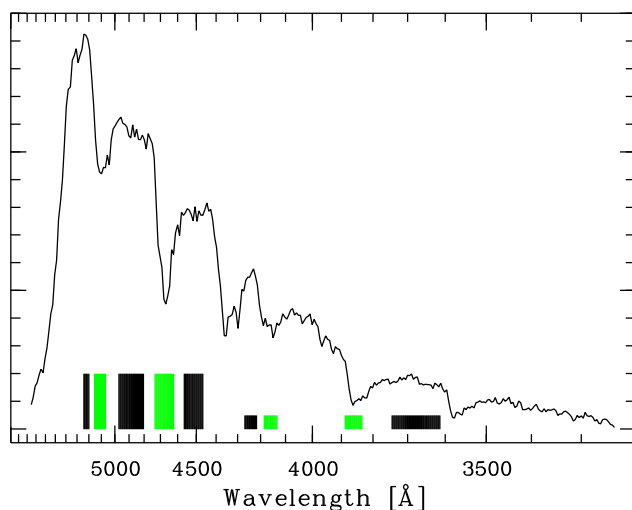


Fig. 1. HES objective prism spectrum of the R-type carbon star CGCS 2954 (Stephenson 1989), illustrating the positions of continuum (black) and band (grey) band-passes defining the C₂ (high boxes) and CN (flat boxes) line indices used for selection in the HES. The abscissa is density above diffuse sky background in arbitrary units. Note that wavelength is *decreasing* towards the right. The sharp drop of the spectra at $\lambda \sim 5400 \text{ \AA}$ is due to the IIIa-J emulsion sensitivity cutoff.

motions for as many objects as possible, and thereby separate the dCs from C giants.

We note that carbon-enhanced, metal-poor stars may be among the FHLC stars presented here. It was recognized by several authors that the fraction of such stars among metal-poor stars rises with decreasing metallicity, reaching $\sim 25\%$ for stars with $[\text{Fe}/\text{H}] < -3.0$, and that carbon overabundances are as high as $[\text{C}/\text{Fe}] = +2.0$ dex (e.g., Norris et al. 1997; Rossi et al. 1999). ¹²C/¹³C isotope measurements of a larger sample of such stars would help to identify the carbon production site(s) at work.

2. Carbon Star Selection

The full HES database consists of ~ 10 million extracted, wavelength calibrated spectra. The input catalog for extraction of objective-prism spectra is generated by using the Digitized Sky Survey I (DSS I). An astrometric transformation between DSS I plates and HES plates yields, for each object in the input catalog, the location of its spectrum on the relevant HES plate, and provides a wavelength calibration zero point (Wisotzki et al. 2000).

Carbon stars can be identified in the HES data base by their strong C₂ and CN bands. We select carbon star candidates when the mean signal-to-noise ratio (S/N) in the relevant wavelength range is > 5 per pixel and both of the C₂ bands $\lambda\lambda 5165, 4737$, or both of the CN bands $\lambda\lambda 4216, 3883$ are stronger than a selection threshold. Band strengths are measured by means of line indices – ratios of the mean photographic densities in the

Table 1. Wavelengths of passbands used for computation of C band indices in the HES. ‘cont’=continuum; ‘flux’=feature passband.

Passband	Use for band index			
	C ₂ 5165	C ₂ 4737	CN 4216	CN 3883
5190–5240 Å	cont			
5060–5150 Å	flux			
4800–4970 Å	cont	cont		
4620–4730 Å		flux		
4460–4560 Å		cont		
4210–4270 Å			cont	
4130–4180 Å			flux	
3830–3890 Å				flux
3610–3740 Å				cont

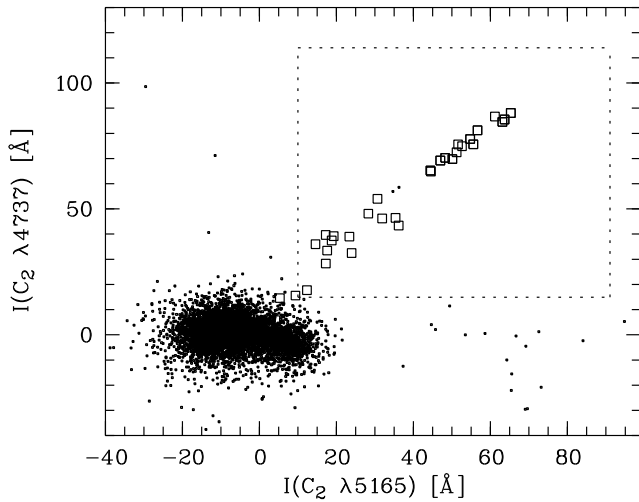


Fig. 2. Selection of carbon stars in the $I(C_2 \lambda 5165)$ versus $I(C_2 \lambda 4737)$ plane. Band strengths are measured by line indices. ‘.’ – all spectra on a randomly chosen HES plate, ‘□’ – test sample of known FHLC stars present on HES plates (see Tab. 4), dashed box – selection region. Spectra in which only *one* high C₂ band index value was measured suffer either from an overlapping spectrum, or from a plate artifact. The selection in the $I(CN \lambda 4216)$ versus $I(CN \lambda 3883)$ plane is done analogously. The two test sample objects outside the selection box are CGCS 525 and CGCS 3180. They are selected by CN band indices (see Tab. 4).

carbon molecular absorption features and the continuum bandpasses shown in Fig. 1, and listed in Tab. 1. The use of *pairs* of indices prevents confusion with plate artifacts, e.g., scratches. It is very unlikely that two such artifacts are present at the positions of two molecular bands. Selection boxes in the $I(C_2 \lambda 5165)$ versus $I(C_2 \lambda 4737)$ and $I(CN \lambda 4216)$ versus $I(CN \lambda 3883)$ planes were chosen well-separated from the dense locus of “normal” stars (see Fig. 2). The selection criteria are listed in Tab. 2.

Table 2. Carbon star selection criteria. The maximum allowed band index values correspond to an integrated density of zero in the feature passbands. That is, larger band indices can only be due to artifacts, e.g. scratches, causing photographic densities (above skybackground) < 0 . Stars are selected if both of their C₂ indices or both of their CN indices fall into the indicated ranges

Feature	Index range [Å]
C ₂ λ 5165	[10,91]
C ₂ λ 4737	[15,114]
CN λ 4216	[2,56]
CN λ 3883	[13,55]

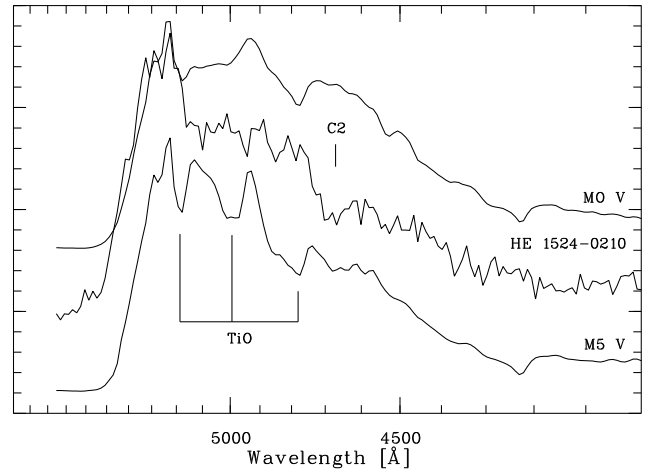


Fig. 3. Comparison of HES spectra of the C star HE 1524–0210, exhibiting a weak C band only, with two M stars. The abscissa is the same as in Fig. 1.

Carbon stars can be distinguished reliably from other late type stars, e.g. M or S stars, even if only weak C bands are present in their spectra (cf. Fig. 3). Other potential sample contaminants are white dwarfs of type DQ, which show carbon molecular bands. However, since the latter usually have a much bluer continuum (see Fig. A.1), they can easily be recognized by visual inspection of the spectra, and by their $U - B$ color. McCook & Sion (1999) list 49 DQs, of which 30 have an available $U - B$ measurement. The average $U - B$ of those is -0.58 , i.e., ~ 1.5 mag away from the average $U - B$ of the HES C star sample. Our $U - B$ colors are measured directly from the HES spectra with a mean accuracy of $\sigma_{U-B} = 0.09$ mag (Christlieb et al. 2001, hereafter Paper I). The average $U - B$ of HES C stars is ~ 0.9 , more than 90% have $U - B > 0.5$, and there is *no* C star of $U - B < 0$ in the HES sample. While 4 (i.e., 13%) of the 30 DQs with $U - B$ in McCook & Sion (1999) have $U - B > 0.0$, the pressure-broadened features of DQs are easily distinguished by visual inspection of the carbon bands (see Fig. A.1).

With a rough estimate of their surface density, we can quantify an upper limit for the contamination of the HES

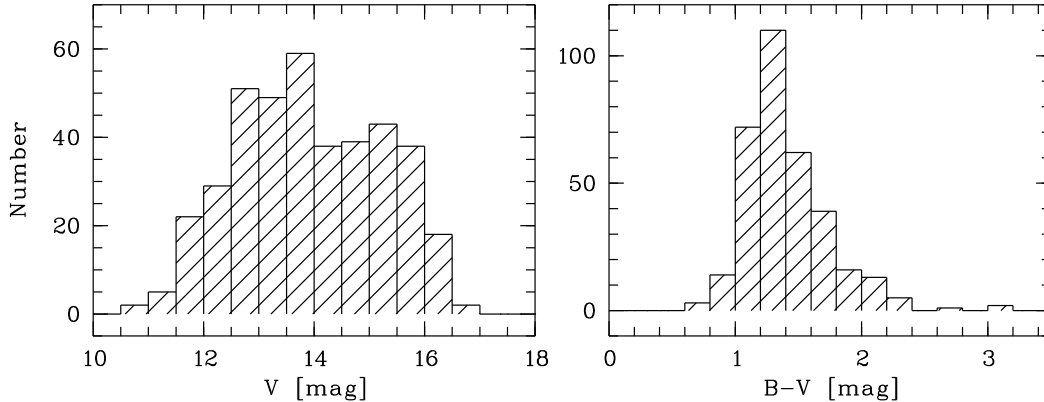


Fig. 4. V magnitude and $B - V$ distribution of the HES FHLC sample. $B - V$ was derived from HES spectra with the procedures described in Paper I.

C star sample by “red” ($U - B > 0.0$) DQs. First of all, we have to take into account that the ratio of northern hemisphere to southern hemisphere DQs is unbalanced in McCook & Sion (1999), as much as the *total* catalog is. This is because the southern hemisphere so far has been surveyed less extensively for white dwarfs. Assuming that the northern hemisphere sample of DQs is complete, we derive a surface density of 9 DQs brighter than $V = 16.5$ in $20\,000\text{ deg}^2$, i.e. $4.5 \cdot 10^{-4}\text{ deg}^{-2}$. Hence, the surface density of $U - B > 0.0$ DQs is $5.9 \cdot 10^{-5}\text{ deg}^{-2}$, and we expect 0.44 DQs to be present on all 329 plates currently used for the exploitation of the stellar content of the HES. Therefore, even if we assume that the sample of DQs known so far is incomplete by a factor of 2, we statistically expect less than 1 DQ to be present in the HES C star sample.

On the 329 HES plates (effective area $6\,400\text{ deg}^2$) we found 403 FHLCs. 90 of them were selected by C_2 band indices only, 171 by CN band indices only, and 144 by C_2 and CN indices. The V and $B - V$ distributions are displayed in Fig. 4. The faintest objects have $V \sim 16.5$, and the most distant objects reach $\sim 35\text{ kpc}$ (cf. Fig. 5), assuming they are all giants with $M_V = -1\text{ mag}$.

3. Testing the Automated Selection

We tested the automated selection extensively and by various methods. In Sect. 3.1 we investigate the selection efficiency. In Sect. 3.2 we derive plate-by-plate selection probabilities for halo dCs on HES plates by simulations. The results of tests with “real” objects are given in Sect. 3.3.

3.1. Selection Efficiency

An important criterion for the evaluation of the quality of a selection algorithm is the *selection efficiency*, i.e. the fraction of desired stars in the raw candidate sample. Tab. 3 summarizes the results. Our selection is very efficient. The low fraction of artifacts demonstrates that the usage of *pairs* of C_2 bands and CN bands indeed very reliably excludes artifacts from selection. However, a con-

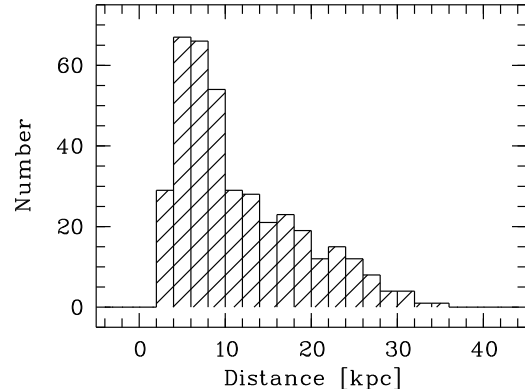


Fig. 5. Distance distribution of the 393 HES FHLCs with available V magnitudes, assuming that they are all giants with $M_V = -1\text{ mag}$.

Table 3. Selection efficiency for C stars in the HES. UNID=*probable* C stars with weak C bands, OVL=overlapping spectra, ART=artifacts, NOIS=very noisy spectra, SAT=saturated spectra. The raw candidate reduction factor is the factor by which the selection algorithm reduces the *total* set of 3 437 630 overlap-free HES spectra with $S/N > 5$ present on 329 HES plates.

Raw candidate reduction factor	1/2900
C stars	31.6 %
UNID	7.0 %
OVL	29.2 %
ART	8.7 %
NOIS	3.8 %
SAT	15.6 %

siderable number of overlapping spectra (overlaps) are selected. Overlaps are detected by an automatic overlap detection algorithm in the HES, using the direct plate data

of the DSS I. It appears that our carbon star selection technique is very sensitive in finding the small number of overlaps not detected by the automatic algorithm.

3.2. Decrease of Selection Probability for Halo dCs

In the HES, some care must be taken when objects with large proper motion are selected. This is because the input catalog for extraction of objective prism spectra is generated by using the DSS I. The dispersion direction of the HES spectra is along declination. Therefore, large proper motions and/or large epoch differences between HES and DSS I plates (13.5 years on average) may result in an offset of the wavelength calibration zero point, leading to smaller C band values, and/or non-detection of objects in the HES, if $\mu_\alpha \Delta t_{\text{HES-DSS I}} \gtrsim 4''$, i.e., > 3 pixels. Offsets of $\mu_\alpha \Delta t_{\text{HES-DSS I}} < 4''$ can be recovered by the spectrum extraction algorithm. Note however that proper motions of a typical halo object ($\langle u \rangle = \langle w \rangle = 0$ km/s; $\langle v \rangle \sim 200$ km/s) result in $\sim 2 \times$ larger offsets along declination than in R.A., since the galactic plane is tilted by 62.6° with respect to the equatorial coordinate system.

In order to estimate how many dCs are expected to be missed in our survey due to the epoch difference problem, we carried out a simulation study in which the plate-by-plate selection function for halo dCs was determined. The simulation is similar to that described in Green et al. (1992). We employ a sample of simulated dCs with halo kinematics, as given by Norris (1986). For the solar neighborhood, he gives

$$v_{\text{rot}} = 37 \pm 10 \text{ km/s} \iff \langle v \rangle = -187 \text{ km/s}, \quad (1)$$

and he determined the velocity ellipsoid to be

$$\sigma_u = 131 \pm 6 \text{ km/s} \quad (2)$$

$$\sigma_v = 106 \pm 6 \text{ km/s} \quad (3)$$

$$\sigma_w = 85 \pm 6 \text{ km/s}. \quad (4)$$

In each simulation we constructed 100 random velocity vectors (u, v, w) , with components following Gaussian distributions according to the above parameters. These velocity vectors were each applied to stars located at the center of the plate under investigation, and converted to proper motions assuming distances d . These were computed from the apparent V magnitude distribution of a sample of 86 C stars without significant p.m. (see Fig. 4), and assuming $M_V = +10$ for dwarf carbon stars. This yields $86 \cdot 100 = 8600$ simulated stars. We compute the position of the star after the time $\Delta t_{\text{HES-DSS I}}$, the epoch difference between DSS I and HES plate, and derive proper motions μ_α, μ_δ from the position differences. We then select the subsample of the 8600 stars with $\mu_\alpha \Delta t_{\text{HES-DSS I}} < 4''$.

As a test sample for an investigation of the dependence of the selection probability on $\mu_\delta \Delta t$, we used a sample of 78 C stars from 44 HES plates *without* significant p.m., as measured in a follow-up campaign carried out in April at ESO, using the Wide Field Imager attached to the MPG/ESO 2.2 m telescope (Christlieb et al. 2001, in

preparation). The stars were shifted in 1 pixel ($= 1''/35$) steps through the range $-700 \mu\text{m} < x < +700 \mu\text{m}$, corresponding to $-47''/25 < \mu_\delta \Delta t < 47''/25$. At each shift step, the selection algorithms were applied.

By applying the selection probability (a function of $\mu_\delta \Delta t$) to the subsample of the 8600 stars with $\mu_\alpha \Delta t_{\text{HES-DSS I}} < 4''$, we determine the fraction of stars which would be detected in the HES *and* selected by our selection algorithm. On the 329 stellar HES plates, 21.4% of the simulated halo dCs are detected and selected.

Green et al. (1992) found that 13% of their C stars are dwarfs. Applying this estimate to our sample, and taking into account that we find only $\sim 20\%$ of the dCs detectable on the HES plates, we estimate that 10–15 out of our 403 FHLCs are dCs. However, since our sample is biased to low-p.m., it is likely that not all of these can be *proven* to be dCs by their large transverse velocity. Based on our simulations we estimate that additional ~ 40 dCs would be detectable on the HES plates, but are currently missed due to the epoch difference problem. This incompleteness will be addressed in a later paper focusing on dC stars in the HES.

3.3. Tests with Known C Stars

We also compiled a test sample of known dwarf and giant C stars present on HES plates (see Tab. 4). We took all three dCs in the southern hemisphere listed by Deutsch (1994), i.e. LHS 1075, G77–61, and KA 2. The (possible) dCs of Warren et al. (1993), having $B_J > 20$, unfortunately are by far too faint to be detectable on HES plates. Cross-identification with the C star lists of Slettebak et al. (1969), Stephenson (1989), Bothun et al. (1991), and Totten & Irwin (1998), yielded 21 stars. Another 6 spectra were produced from slit spectra with the procedures described in Paper I.

In our test, *all* 21 stars not known as dwarfs were selected either by their strong C₂ bands, or their CN bands. The simulated spectra were also *all* selected. Of the three dCs, one (KA 2) was selected, and the other two (G77–61, LHS 1075) not. From these results we conclude that our sample of giant C stars and dwarfs with low p.m. (e.g. dCs belonging to the disk population) is highly complete. From the small number of dCs in our test sample we are not able to draw any definitive conclusions, but our results suggest that only a minor fraction of the halo dCs are detected in the HES. This is consistent with $\sim 20\%$ of the simulated halo dCs being found (see Sect. 3.2).

4. The Surface Density of C Stars

In an effective area of 6400 deg^2 (329 of 380 the HES plates; for a description how the effective area is estimated see Wisotzki et al. 2000), we have isolated a total of 403 C stars. A straightforward estimate of the surface density of FHLC stars we detect with the HES is hence obtained from the ratio of these two numbers, yielding 0.063 deg^{-2} . However, one has to take into account that the effective

Table 4. Test sample of dwarf and giant C stars present on HES plates. Sources: BEM91=Bothun et al. (1991), D94=Deutsch (1994), S89=Stephenson (1989), SKB69=Slettebak et al. (1969), TI98=Totten & Irwin (1998). Stars marked with TI98 have been recently reported by Totten et al. (2000) to have no significant p.m. Therefore, we list them with $(\mu_\alpha \Delta t, \mu_\delta \Delta t) = (0, 0)$. KA 2 was not selected by CN bands, using its real spectrum, but it *was* selected in the course of our simulations. This is because the S/N at the position of the CN bands is too low in the former spectrum, and effectively infinite in the simulated spectrum

Name	HE Name	B_J	$B - V$	$\mu_\alpha \Delta t$	$\mu_\delta \Delta t$	Selected by			Source
						C ₂	CN	All	
CGCS 39	HE 0017+0055	(sat.)				1	1	1	S89
SKB 2	HE 0039-2635	13.1	1.1			1	1	1	SKB69
BEM91 23	HE 0100-1619	15.9	1.5			1	0	1	BEM91
CGCS 177	HE 0106-2837	13.8	2.1			1	0	1	S89
SKB 5	HE 0111-1346	13.3	1.4			1	1	1	SKB69
0207-0211	HE 0207-0211	15.5	2.2	0.0	0.0	1	0	1	TI98
BEM91 08	HE 0228-0256	16.2	2.0			1	0	1	BEM91
CGCS 525	HE 0330-2815	13.8	1.5			0	1	1	S89
CGCS 935	HE 0521-3425	13.0	1.3			1	1	1	S89
0915-0327	HE 0915-0327	14.5	2.3	0.0	0.0	1	0	1	TI98
1019-1136	HE 1019-1136	15.2	1.8	0.0	0.0	1	0	1	TI98
CGCS 2954	HE 1104-0957	(sat.)				1	1	1	S89
CGCS 3180	HE 1207-3156	12.8	1.2			0	1	1	S89
CGCS 3274	HE 1238-0836	(sat.)				1	1	1	S89
1254-1130	HE 1254-1130	16.1	2.2	0.0	0.0	1	0	1	TI98
1339-0700	HE 1339-0700	15.0	1.7	0.0	0.0	1	0	1	TI98
1442-0058	HE 1442-0058	17.8	2.2	0.0	0.0	1	0	1	TI98
CGCS 5435	HE 2144-1832	12.6	1.4			0	1	1	S89
CGCS 5549	HE 2200-1652	12.3	0.9			1	1	1	S89
2213-0017	HE 2213-0017	16.4	2.4	0.0	0.0	1	0	1	TI98
2225-1401	HE 2225-1401	16.5	2.9	0.0	0.0	1	0	1	TI98
CLS 50				0.0	0.0	1	0	-	Simul.
CLS 31				0.0	0.0	1	1	-	Simul.
CLS 54				0.0	0.0	1	1	-	Simul.
KA 2				0.0	0.0	1	1	-	Simul.
B1509-0902				0.0	0.0	1	1	-	Simul.
UM 515				0.0	0.0	1	0	-	Simul.
LHS 1075	HE 0023-1935	16.1	1.4	-0''24	-10''0	0	0	0	D94
KA 2	HE 1116-1628	16.6	1.3	-0''21	0''24	1	0	1	D94
G77-61	HE 0330+0148	15.0	1.4	1''9	-7''5	0	0	0	D94

area accessible on average for each object depends on its brightness, since the HES limiting magnitude varies from plate to plate. For example, the effective area for an object as faint as $B = 17.0$ is only 73% of the overall survey area, mainly because only 254 of the contributing plates reach this magnitude (see Fig. 2 in Wisotzki et al. 2000). An additional brightness dependence is caused by the fact that faint objects are more easily affected by overlapping spectra than bright objects. We therefore determine the FHLC surface density as follows:

$$\text{surface density} = \sum_{i=1}^{403} \frac{1}{\text{effarea}(B_J)_i}, \quad (5)$$

where $\text{effarea}(B_J)$ was determined as described in Wisotzki et al. (2000). We obtain a FHLC surface density of $0.072 \pm 0.005 \text{ deg}^{-2}$ on the 329 HES plates we used.

5. Discussion and Conclusions

In an effective area of $6\,400 \text{ deg}^2$ we have isolated a total of 403 C stars. Our efforts have thus already increased the number of known FHLC stars by a factor of nearly five.

We find almost quadruple the surface density of carbon stars compared to the surveys summarized by Green et al. (1994). Since those previous surveys claimed limiting magnitudes about 1.5 mag fainter than the HES, this highlights the greatly enhanced selection sensitivity of FHLC stars in the HES, which is more sensitive to a variety of C₂ or CN molecular absorption band strengths. Automated selection techniques may be superior to visible inspection of objective-prism spectra with binocular microscopes, as done e.g. in the survey of Sanduleak & Pesch (1988). Photometric surveys for C stars have generally selected red objects only, which preferentially selects mostly the much less common high latitude AGB stars. Margon et al. (2000) report a FHLC star surface density

of “at least” 0.04 deg^{-2} in the SDSS. This is still almost a factor of 2 below our value, and again, the SDSS is much deeper than the HES ($r' < 19.5$).

Due to an average epoch difference of 13.5 years between DSS I and HES plates, we expect to detect and select only $\sim 20\%$ of the halo dCs that we could detect and select if direct plates had been taken simultaneously with the HES plates. Our simulations indicate that 10–15 out of the 403 FHLCs published in this paper are dCs. Note, however, that this number is uncertain, because the kinematics of halo dCs is not precisely known. We estimate that additional ~ 40 dCs are detectable on the HES plates, but are currently missed due to the epoch difference problem. We are extending the current sample to include proper-motion corrected input catalogs for the extraction of HES spectra, to find *all* dCs, and other objects that can have large proper motions, like halo white dwarfs.

Acknowledgements. We thank D. Koester for providing model spectra of DQs, and C. Fechner for technical support in preparing this article. This work was partly supported by Deutsche Forschungsgemeinschaft under grant Re 353/40. P.J.G. acknowledges support through NASA Contract NAS8-39073 (ASC).

References

- Bothun, G., Elias, J. H., MacAlpine, G., et al. 1991, *AJ*, 101, 2220
 Brewer, J. P., Richer, H. B., & Crabtree, D. R. 1996, *AJ*, 112, 491
 Christlieb, N., Wisotzki, L., Reimers, D., et al. 2001, *A&A*, 366, 898 (Paper I)
 Dahn, C. C., Liebert, J., Kron, R. G., et al. 1977, *ApJ*, 216, 757
 Deutsch, E. W. 1994, *PASP*, 106, 1134
 Eggen, O. J., Lynden-Bell, D., & Sandage, A. R. 1962, *ApJ*, 136, 748
 Green, P. J., Margon, B., & Anderson, S. F. 1992, *ApJ*, 400, 659
 Green, P. J., Margon, B., Anderson, S. F., et al. 1994, *ApJ*, 434, 319
 Green, P. J., Margon, B., & MacConnell, D. J. 1991, *ApJ*, 380, L31
 Heber, U., Bade, N., Jordan, S., et al. 1993, *A&A*, 267, L31
 Ibata, R. A., Gilmore, G., & Irwin, M. J. 1994, *Nature*, 370, 194
 Johnston, K. V., Zhao, H., Spergel, D. N., et al. 1999, *ApJ*, 512, L109
 Liebert, J., Schmidt, G. D., Lesser, M., et al. 1994, *ApJ*, 421, 733
 MacAlpine, G. M. & Williams, G. A. 1981, *ApJS*, 45, 113
 MacAlpine, G. M. & Lewis, D. W. 1978, *ApJS*, 36, 587
 Majewski, S. R., Ostheimer, J. C., Kunkel, W. E., et al. 2000, *AJ*, 120, 2550
 Margon, B., Anderson, S. F., Williams, B. F., et al. 2000, in *AAS Meeting*, Vol. 197, 1309
 McCook, G. P. & Sion, E. M. 1999, *ApJS*, 121, 1

- Norris, J. 1986, *ApJS*, 61, 667
 Norris, J. E., Ryan, S. G., & Beers, T. C. 1997, *ApJ*, 488, 350
 Reimers, D. & Wisotzki, L. 1997, *The Messenger*, 88, 14
 Rossi, S., Beers, T. C., & Sneden, C. 1999, in *ASP Conf. Ser.*, Vol. 165, *The Third Stromlo Symposium: The Galactic Halo*, ed. B. Gibson, T. Axelrod, & M. Putman, 264–268
 Sanduleak, N. & Pesch, P. 1988, *ApJS*, 66, 387
 Searle, L. & Zinn, R. 1978, *ApJ*, 225, 357
 Slettebak, A., Keenan, P. C., & Brundage, R. K. 1969, *AJ*, 74, 373
 Stephenson, C. B. 1989, *Publ. W.&S. Obs*, 3
 Totten, E. J. & Irwin, M. J. 1998, *MNRAS*, 294, 1
 Totten, E. J., Irwin, M. J., & Whitelock, P. A. 2000, *MNRAS*, 314, 630
 Warren, S. J., Irwin, M. J., Evans, D. W., et al. 1993, *MNRAS*, 261, 185
 Wisotzki, L., Christlieb, N., Bade, N., et al. 2000, *A&A*, 358, 77
 Wisotzki, L., Köhler, T., Groote, D., et al. 1996, *A&AS*, 115, 227

Appendix A: HES example spectra of C stars

Appendix B: The HES FHLC sample

In Tab. B.1 we list the sample of 403 HES FHLC stars described in this paper. The table is made available only electronically. It contains the following columns:

hename	HE designation
ra2000	R.A. at equinox 2000.0, derived from DSS I
dec2000	Declination at equinox 2000.0, derived from DSS I
field	ESO-SERC field number
plate	HES plate number
q	Plate quarter
objtyp	Object type (stars/bright/ext)
B _J	<i>B_J</i> magnitude
V	<i>V</i> magnitude
<i>B</i> − <i>V</i>	<i>B</i> − <i>V</i> magnitude, derived from HES spectra
<i>U</i> − <i>B</i>	<i>U</i> − <i>B</i> magnitude, derived from HES spectra
C2idx1	Band index of C ₂ 5165 Å
C2idx2	Band index of C ₂ 4737 Å
CNidx1	Band index of CN 4216 Å
CNidx3	Band index of CN 3883 Å
selC2	C ₂ band index selection flag
selCN	CN band index selection flag

B_J magnitudes are accurate to better than $\pm 0.2 \text{ mag}$, including zero point errors (Wisotzki et al. 2000). *V* magnitudes were derived by the procedures described in Paper I. The object types “stars”, “bright” and “ext” refer to point sources, sources above a saturation threshold, and sources detected as extended in DSS I images, respectively. We do not list *V*, *B* − *V* and *U* − *B* for saturated objects, because our color calibrations are not valid for them.

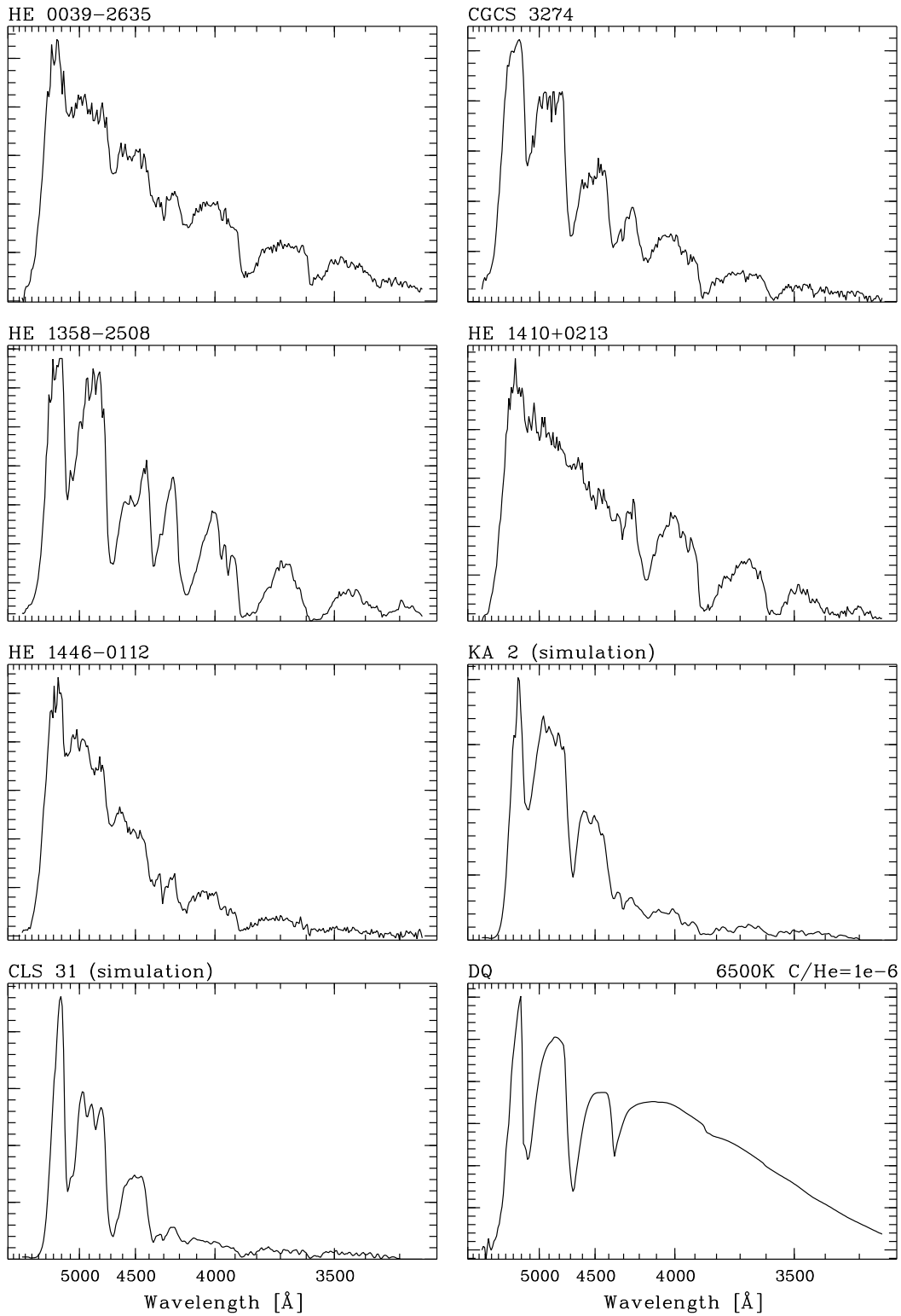


Fig. A.1. HES spectra of a representative sample of seven C stars, displaying a variety of C₂ and CN band strengths. The spectra of KA 2 and CLS 31 were converted to objective-prism spectra from slit spectra with the procedures described in Paper I. For comparison, the spectrum of a DQ white dwarf with $T_{\text{eff}} = 6500\text{K}$ and $\text{C/He} = 10^{-6}$ is shown in the lower right panel. That star has $U - B = -0.6$.